C. R. Mecanique 340 (2012) 668–677

Contents lists available at SciVerse ScienceDirect

Comptes Rendus Mecanique

www.sciencedirect.com

Damage detection on hollow cylinders by Electro-Mechanical Impedance method: Experiments and Finite Element Modeling

Seyed Reza Hamzeloo [a,b], Mahnaz Shamshirsaz [a,*], Seyed Mehdi Rezaei [a,b]

[a] New Technologies Research Center, Amirkabir University of Technology (Tehran Polytechnic), 424 Hafez Avenue, Tehran, Iran
[b] Mechanical Engineering Department, Amirkabir University of Technology (Tehran Polytechnic), 424 Hafez Avenue, Tehran, Iran

ARTICLE INFO

Article history:
Received 30 May 2012
Accepted 2 July 2012
Available online 24 July 2012

Keywords:
Solids and structures
Electro-Mechanical Impedance (EMI)
Damage detection
Hollow cylinder
Finite Element Modeling (FEM)
Damage orientation
Structural stiffness

ABSTRACT

Damage detection using the Electro-Mechanical Impedance method (EMI) is based on measuring the electrical impedance spectrum of piezoelectric wafer active sensors (PWAS) attached to the structure. Any changes in the structure, such as a crack, lead to changes in the mechanical impedance of the structure, which affect the PWAS electrical impedance by the electromechanical coupling effect of PWAS. The motivation here is to examine the performance of the EMI technique for damage detection on hollow cylinders. For this purpose, the EMI technique on hollow cylinders was implemented experimentally. Damage detection was realized by comparison of damage metrics extracted from measured PWAS electrical impedance for undamaged and damaged cylinders. A Finite Element Model (FEM) of a hollow cylinder considering the EMI technique has been developed. FEM results are in accordance with experimental data and similar trends are also observed for damage metrics. The influence of different damage types and damage location on damage metrics has been explored both by experiments and FEM. Moreover, the effects of accumulated damage on damage metrics are explored both by FEM and experiments. To examine the influence of host material stiffness on damage metrics, the EMI technique was performed on aluminum and steel hollow cylinders with different thicknesses.

1. Introduction

Impedance-based Structural Health Monitoring (ISHM) using piezoelectric wafer active sensors (PWAS) has been extensively developed as a damage detection method in structures [1]. PWAS is excited with a high-frequency sweep, the electrical impedance of PWAS is monitored simultaneously in order to recognize any changes in the structural mechanical impedance [2]. Mechanical impedance that affects electrical impedance of PWAS, is the ratio of excitation force and induced velocity. Any changes in the stiffness of structure will influence the monitored impedance spectrum. The extraction of these changes will therefore reveal the existence of damage in the structure. Application of a relatively high frequency range to PWAS makes the impedance measurements more sensitive to local and global changes in the system [3]. In fact, while the stiffness of the structure is changed, the PZT will draw more or less current with the same applied voltage. The Electro-Mechanical Impedance (EMI) type model for a PZT-structure interaction system was first proposed by Liang et al. [4]. An equation was presented for a single degree-of-freedom model. It consisted of the electrical admittance of a PZT attached on a host structure. When the impedance is varied over a range of frequencies (10–400 kHz), plots of real or imaginary parts of impedance or inductance relating to the health of a structure can be obtained [1]. The real part of PWAS electrical impedance is more sensitive to the variation of structural stiffness. Hence this has been used for ISHM in more studies.

* Corresponding author.
E-mail address: shamshir@aut.ac.ir (M. Shamshirsaz).

1631-0721/$ – see front matter
http://dx.doi.org/10.1016/j.crme.2012.07.001

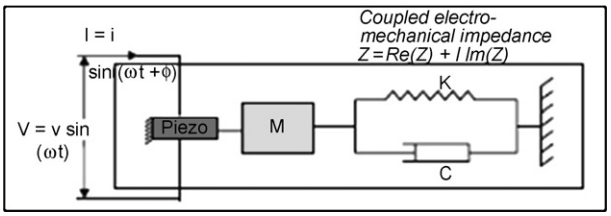

Fig. 1. Coupled 1D electromechanical impedance model presented by Liang et al. [4].

Damage detection was realized by comparison of damage metrics extracted from measured PWAS electrical impedance for undamaged and damaged cylinders. In signal processing, statistical algorithms based on frequency-by-frequency comparisons such as "root-mean-square deviation" (RMSD) are proposed and utilized for damage detection by the EMI technique [3]. The performance of RMSD and other statistical algorithms, such as mean absolute percentage deviation (MAPD), covariance and correlation coefficients as indicators of damage were investigated by Tseng and Naidu [5]. It was reported that RMSD and MAPD could be suitable for characterizing the growth and the location of damage, whereas the covariance and the correlation coefficient are efficient in quantifying the increase in damage size at a fixed location.

Many applications of the EMI method have been focused on beam and plate structures. Giurgiutiu and Zagrai also derived an expression for the EMI admittance and impedance that incorporates both the sensor dynamics and the structural dynamics [6]. Giurgiutiu used this model to predict the EMI response of thin plates and aging aircraft panels [7,8]. It was shown that the real part of impedance is more sensitive to the variation of structural stiffness [6]. Tseng and Bhalla created the concept of effective mechanical impedance to consider the two-dimensional interaction of the PZT patch with the host structure [9,10]. Zhou and Liang derived an analytical solution for a PZT-integrated thin cylindrical shell structure, which was limited to certain boundary conditions [11]. Yang developed this model and also related degradation of strain energy due to a simple damage on the impedance [12]. The EMI of a structure with attached PWAS was modeled by Yang assuming the interaction of host structure with PWAS on its borders on a plate. Yaowen Yang developed this model for cylindrical shells considering whole shape damage [13]. He demonstrated that the most affecting parameters on EMI spectrum are axial and peripheral distances of damages from sensor location.

A few studies have theoretically modeled the damage with simple geometry such as a hole or a slot [7–9,11,13]. For structures with geometrical and material complexity, a theoretical model cannot be developed. Therefore, FEM could not only be applied to model the complex structure but also could model damage in a structure with different forms and geometries. In fact, the coupled field characteristic of FEM in the calculation allows the prediction of structural damage by EMI technique in complicated environmental and working conditions. Tseng et al. used ANSYS to monitor two types of damage, voids and cracks, in a concrete structure [14]. Zagrai and Giurgiutiu used the FEM model to extract the EMI of an aluminum square, circular plates and damage detection of radial cracks [7]. Peairs et al. used spectral element formulation for damage detection in beam structures [15].

Many researchers have reported the application and modeling of EMI method [1,16]. However, only a few works are focused on the prediction of damage detection in a hollow cylinder using the EMI method. The diverse applications of this method in different industries such as petrochemical, oil and gas are vast.

In the present work, damage detection in hollow cylinders is explored using the EMI technique. FEM and experiments are used to extract the electrical impedance spectrum of PWAS. The results show that the simulation data are in accordance with experimental results. The FEM proposed and developed in this study is able to predict the EMI spectrum for healthy and damaged cylinders and consequently to obtain the damage metrics. Intensity of damage is increased by insertion of different type of damage in different locations sequentially. The RMSD algorithm is used to extract the damage metrics from impedance spectra for damage detection. The influence of damage states, material and geometrical characteristics on extracted damage metrics is investigated both by FEM and experimental tests. Damage detection in two different materials: steel and aluminum, in a hollow cylinder with different thicknesses is studied. Moreover, the effect of damage orientation and damage type on damage metric trends is investigated.

2. Impedance-based structural health monitoring

PWAS is used as high-frequency actuator/sensor in ISHM. Electrical signals from the sensor attached to structure are measured using the coupling effect between the electrical and mechanical impedance of system. Any change in the stiffness of the structure such as damage, material properties, modifies mechanical impedance of structure and consequently affects the electrical impedance of sensor.

EMI of bonded PWAS can be explained simply by the model described in Eq. (1) as presented by Liang et al. [4]:

$$Z(\omega) = \left[\mathrm{j}\omega c \left(1 - k_{31}^2 \frac{Z_{str}(\omega)}{Z_{PWAS}(\omega) + Z_{str}(\omega)} \right) \right]^{-1} \tag{1}$$

where c is the electrical capacitance of the PWAS, $Z_{str}(\omega)$ is the 1-dof structural impedance as seen by the PWAS, and $Z_{PWAS}(\omega)$ is the quasi-static impedance of the PWAS.

Table 1
Material properties of PZT type 5H4E used as actuator/sensor in FEM as in experiments (Piezo Systems, Inc.).

Property	Symbol	Value
Relative dielectric constant	KT3	3800 kHz
Piezoelectric strain coefficient	d33	650×10^{-12} m/V
	d31	-320×10^{-12} m/V
Piezoelectric voltage coefficient	g33	19.0×10^{-3} V m/N
	g31	-9.5×10^{-3} V m/N
Coupling coefficient	k33	0.75
	k31	0.44
Polarization field	Ep	1.5×10^{6} V/m
Initial depolarization field	Ec	3.0×10^{5} V/m
Mechanical density	ρ	7800 kg/m^3
Mechanical Q		32
Elastic modulus	YE3	5.0×10^{10} N/m^2
	YE1	6.2×10^{10} N/m^2
Thermal expansion coefficient		$\sim 3 \times 10^{-6}$ m/m °C

Mechanical impedance of a structure is related to the mode functions and natural frequencies of the structure and is simply defined by ratio of an applied force to the resulting velocity.

It is clear that this is a 1D model of PWAS and cannot be applied or generalized for all cases.

3. FEM modeling

In order to study the effect of damage on the sensor response, a coupled-field FEM in EMI technique was developed using ABAQUS. In fact, FEM permits the computation of electrical reaction charges over each sensor electrode, employed to derive the corresponding EMI signature. The resulting impedance spectrum is then processed to calculate the damage metrics. A constant voltage is applied in harmonic analysis which represents a sweep of frequency in simulation. A constant voltage of 1 V is applied to the top surface of PWAS and a zero voltage to bottom surface nodes. The piezo actuator/sensor is modeled with a piezoelement type C3D8E. The material properties of PZT are given in Table 1.

As the sweep of frequency is applied to the model, a complex nodal electric charge can be collected from the top surface of PWAS. This is carried out in experiment with a self-sensing circuit. Then, related electrical current at each frequency can be calculated from the collected electrical charge using Eq. (2):

$$I(j\omega) = i.\omega.Q(j\omega) \tag{2}$$

The electromechanical impedance of system is obtained by Eq. (3):

$$Z(j\omega) = V(j\omega)/I(j\omega) \tag{3}$$

The real part of impedance that is more sensitive to the changes in impedance signature is extracted and a comparison of electromechanical impedance spectroscopy of healthy and damaged cases is implemented [2,3,17]. The result of comparison is revealed by a damage index or metric. Fig. 2 shows the real part of impedance for a free PZT (non-attached) with dimensions $7 \times 7 \times 0.27$ mm. FEM impedance spectrum of a free PWAS obtained by simulation shows a good accordance in frequency range of 0 to 1 MHz with experiments carried out by Giurgiutiu [17].

Fig. 3 shows a model of attached PWAS on a hollow cylinder. It should be noted that selection of an inappropriate mesh size leads to an incorrect effect on the excitation modes which consequently results to an inaccurate impedance spectrum.

In fact, the mesh size should be smaller than the wavelength of sound speed in the material. Therefore, the effect of time increment of stress wave passing through the element should be considered. The sound velocity in material and stress wavelength is related to the sound speed in material by Eqs. (4) and (5):

$$C_L = \sqrt{\frac{E(1-\nu)}{\rho(1-2\nu)(1+\nu)}} \tag{4}$$

$$\lambda = c_L.dt \tag{5}$$

where C_L is the sound velocity in material, E is Young's modulus, ν is Poisson's ratio, ρ is density, dt is minimum time increment and λ is the wavelength. Using a minimum of 15 elements per wavelength, limits wave dispersion errors to less than 1% [18].

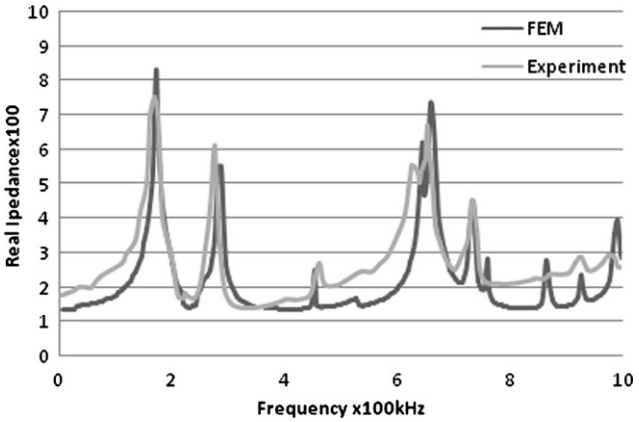

Fig. 2. Impedance spectrum of a free PZT: comparison of simulation results with experimental data reported in the literature [17].

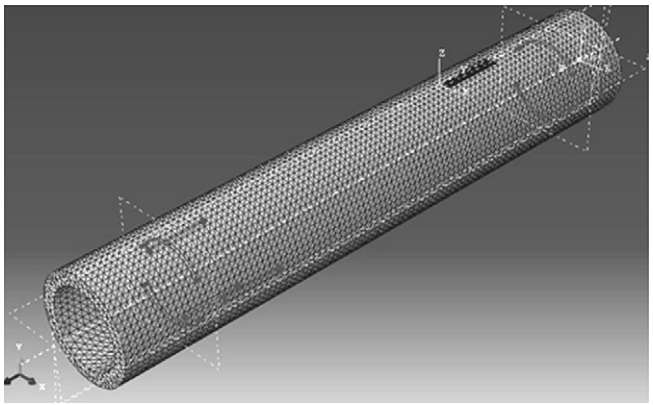

Fig. 3. Finite Element Model of a hollow cylinder with attached PWAS with the existence of damages on inner wall.

Table 2
Wave speed and mesh size for different materials used in FEM.

Material	PZT5H(d31)	Aluminum	Steel
Wave speed (m/s)	3281	6197	5860
Maximum mesh size (m)	0.00218	0.00415	0.00391
Selected mesh size (mm)	1.75	3.5	3.5

The mesh size is chosen smaller than the calculated wavelength and is selected related to the frequency sweep range. The term dt is the minimum time period in the time domain signal. The wave speed and mesh size for different materials used in FEM are presented in Table 2.

A finer mesh is selected for PWAS in order to collect the charge density with more precision from PWAS nodes. Boundary nodes of PWAS are overlapped with the adjacent nodes of host structure.

First, the frequency sweep is emitted from 10 to 100 kHz as performed in experiments. Then, in order to assure a maximum amount of peak density in the resulted spectrum, the frequency sweep range is reselected for the further tests from 10 to 40 kHz. Before selecting the appropriate mesh size for each model, a frequency analysis is performed to guarantee the excitation of all modes in the selected frequency range.

An important point in PWAS modeling is to consider frequency-dependent material damping in FEM. The damping of PWAS is related to the permittivity coefficients of PWAS. Also, taking into account the structural damping of cylinder is essential in modeling since the impedance spectrum depends on damages and any changes in the stiffness of structure. The two most conventional damping models are mass-proportional ($\propto 1/\omega$); alpha type and stiffness-proportional ($\propto \omega$); beta type [19]. In the frequency-domain, coefficients are simply chosen to give the required damping at each calculated frequency. Damping coefficients used in FEM are given in Table 3.

Table 3
Assigned damping coefficients in FEM.

Material	PZT5H-4E		Aluminum		Steel	
Damping coefficient	alpha beta	3000 1e–9	structural damping	0.0005	structural damping	0.001

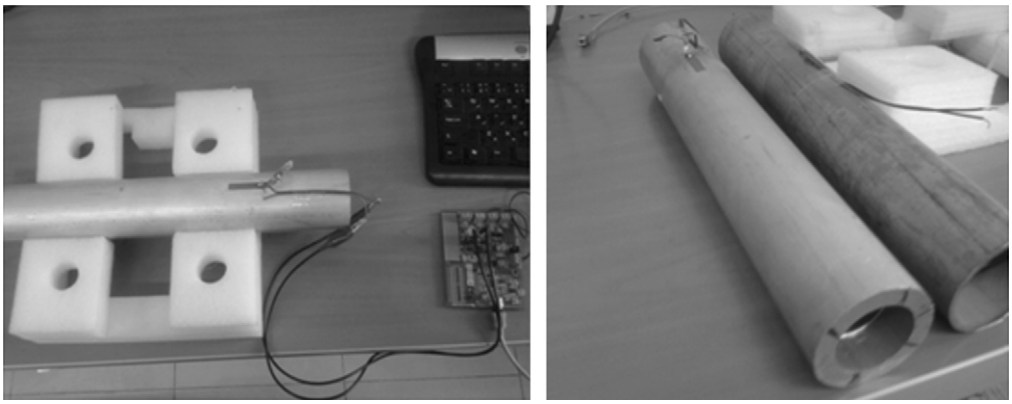

Fig. 4. A) Impedance measurement of hollow cylinder with evaluation board AD5933A; B) aluminum hollow cylinders with 2 mm, 5 mm and 10 mm wall thickness.

Table 4
Specimens used in experiments and FEM.

Name	Dimensions (mm)	Material
Al-thick	$D0 = 60,\ Di = 40,\ L = 350$	aluminum 2025
Al-thin	$D0 = 60,\ Di = 55,\ L = 350$	aluminum 2025
St-thick	$D0 = 60,\ Di = 40,\ L = 350$	stainless steel 304
St-thin	$D0 = 60,\ Di = 55,\ L = 350$	stainless steel 304

4. Experimental tests

4.1. Experimental set-up

As shown in Fig. 4, actuation of attached PWAS and the gathered data is carried out using an evaluation board with a miniaturized AD-5933A chipset. One PWAS of dimensions 30×5 mm and thickness of 0.267 mm was mounted on outer surface of the cylinder, 25 mm apart from the one edge. A frequency range of 10 to 40 kHz was used for the PWAS's self-sensing actuation. The criterion used to select a suitable frequency range is a domain containing more peak density [17,18]. A free–free boundary condition was imposed to cylinders. For this purpose, the cylinders were put on the foam to reduce the contact effects.

4.2. Experimental test specimens

In order to validate the effectiveness of the EMI method for damage detection in pipes and cylinders, the experimental tests detecting different artificial notches in aluminum and steel hollow cylinders were carried out. Four different types of cylinders were used to reveal the effects of thickness and material stiffness on the final results of EMI damage indexes. These test specimens are categorized in Table 4.

First, the baseline impedance was collected from the PWAS for the cylinders supposed as healthy. Then, ten different damage cases; circumferential and longitudinal notches with the same intensity and different locations were sequentially inserted on cylinder, as described in Fig. 5. These circumferential and longitudinal notches were generated artificially in the inner wall of hollow cylinders with a turning machine using an inner tool tip. Longitudinal notches are 25 mm lengths. Circumferential notches with similar lengths cover 54 and 72 degrees of inner wall section in thin and thick cylinders respectively (Fig. 5).

The undamaged cylinder with no notch is indexed 0 in Fig. 5. The damaged cases indexed 1 to 4 is the cylinders with inserted circumferential notches at distance 25 mm from the cylinder edges. Damaged cases indexed 5 to 7 are the cylinders with inserted longitudinal notch at a distance 60 mm from the PWAS sensor. Damage 5 is inserted beneath and opposite side of the sensor location while damages 6 and 7 are at the angles -90 and $+90^\circ$ relative to PWAS location, respectively. Damages 8, 9 and 10 are the duplication of damages 5, 6 and 7, respectively. This means that similar notches were inserted

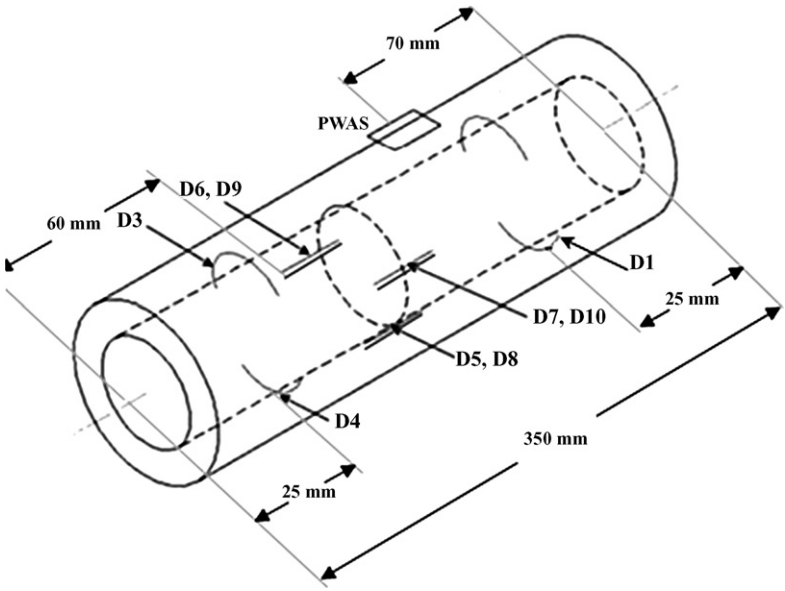

Fig. 5. Schematic of inserted damages (D1 to D10) in the inner wall of hollow cylinders.

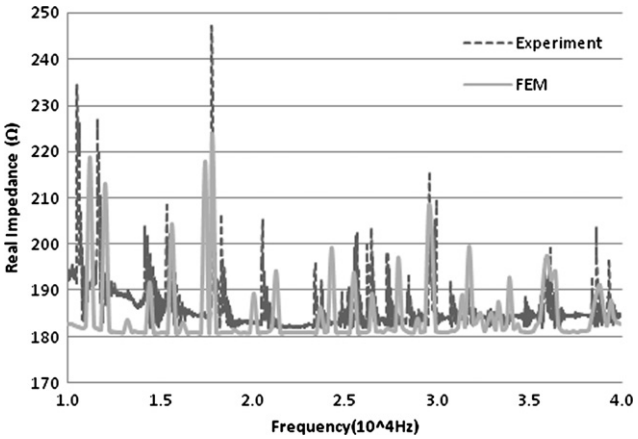

Fig. 6. Comparison of experimental and FEM impedance spectrum for an undamaged aluminum thick cylinder.

1 mm parallel to the damage 5 to 7 positions. After each damage incident, the measurements were carried out by PWAS to obtain impedance spectra.

5. Results and discussions

Fig. 6 shows the comparison of EMI spectra obtained by experiment and by FEM for a thick aluminum hollow cylinder in the frequency range of 10–40 kHz for an undamaged cylinder. As it can be seen, FEM simulation developed in this study could predict the EMI spectrum for hollow cylinders with a satisfactory approximation. The deviation of simulation data from experimental results can be due to applying an imperfect free–free boundary condition in the experiments. This deviation consequently affects the resulted damage metrics. These results can be compared with those presented in Fig. 2. It can be seen that natural frequencies of a bonded PWAS occur at lower frequencies comparing to ones for free PWAS. This was also reported by [17,20].

To explore the influence of damage orientation, damage distance from PWAS and damage type, damages 1 to 10 were inserted individually on an aluminum thick hollow cylinder using FEM (Figs. 3 and 5). The related damage metrics obtained by RMSD algorithm are presented in Fig. 7. RMSD algorithm was extracted using the difference of damaged and undamaged

Fig. 7. RMSD values obtained by FEM for the thick aluminum specimen.

signals by applying Eq. (6). The resulting values can be presented by damage metric bars given in Fig. 7. These damage metrics allow identification of the damaged cases from the intact cylinder by further algorithms (Eq. (6)):

$$RMSD(\%) = \sqrt{\frac{\sum_{i=1}^{i=N}(\mathrm{Re}(Z(\omega_i)) - \mathrm{Re}(Z_0(\omega_i)))^2}{\sum_{i=i}^{i=N}(\mathrm{Re}(Z_0(\omega_i)))^2}} \tag{6}$$

where $Z(\omega_i)$ is the post-damage impedance signature at the i-th measurement point and $Z_0(\omega_i)$ is the undamaged value at the i-th measurement point.

Damages indexed from 1 to 4 are circumferential notches and damages 5 to 7 are longitudinal notches. Damages 8 to 10 are duplication of longitudinal notches inserted parallel to first ones.

The RMSDs resulted from damages 1 to 4 are compared with each other in order to explore the effect of damage orientation. Fig. 5 shows that damages 1 and 4 are located on the opposite sides of the cylinder compared to the PWAS location, while damages 2 and 3 are located on the same side with PWAS. Damages 1 and 4 have significant metric values comparing to those for damages 2 and 3. Damages 1 and 2 are close to PWAS location with the same axial distance while damages 3 and 4 are far from the sensor location. RMSDs of damages 1 and 2 are higher compared to RMSDs of damages 4 and 3, respectively. Therefore, both orientation and longitudinal distance from sensor location affect the damage metrics. Circumferential damage located on the opposite side of PWAS position and near sensor location has a higher effect on the damage metrics.

To investigate the influence of damage type on damage metrics, longitudinal damages 5 to 7 were inserted in the hollow cylinder. The results show that damage metrics of longitudinal damages inserted peripherally closer to the PWAS location (damages 6 and 7) have also greater values comparing to RMSD values related to damage 5. These results are also confirmed by Yang [13]. Yang reported that “the sensitivity of the PZT transducer depends on not only the distance between the damage and the PZT, but also the damage location (peripherally)”.

In fact, changing the location of the damage will alter the vibrational characteristic of the cylinder and thus the PWAS impedance signature and its sensitivity for damage detection. Generally, PWAS is more sensitive to the damage closer to it [2,13].

A combination of damages of different types, locations and positions can generally occur on industrial equipment in service. Therefore, a study on the effect of accumulative damage on a hollow cylinder is needed. For this purpose, ten damages were inserted on hollow cylinders specified in Table 1 as indexed from 1 to 10 in Fig. 5. The impedance signatures obtained experimentally for undamaged and all accumulative damaged cases inserted on Al-thick cylinders are demonstrated in Fig. 8.

In Fig. 8, each curve related to damaged case i, represents the impedance spectrum resulted from damage i accumulated with damages 1 to $i-1$. The difference of each damage curve with undamaged curve is used to calculate the related damage metric using the RMSD algorithm.

The curves in Fig. 9 are obtained using RMSD of impedance spectra obtained from Fig. 8. RMSDs are calculated for each damage state with a baseline of an undamaged cylinder. These results show that RMSD trends obtained by experiments and by FEM are almost similar.

As it can be observed from Fig. 9, accumulating damage from 1 to 10 does not always lead to an increase in RMSD trends. Hence, the progressive problems such as accumulating damages or crack propagation does not lead to an increase in damage metrics obtained by the RMSD algorithm in hollow cylinders, although crack deepening almost led to an increase in damage metrics.

Therefore, it can be deduced that using statistical absolute RMSD algorithm to distinguish the sequentially accumulated damages becomes difficult for hollow cylinders [5,8].

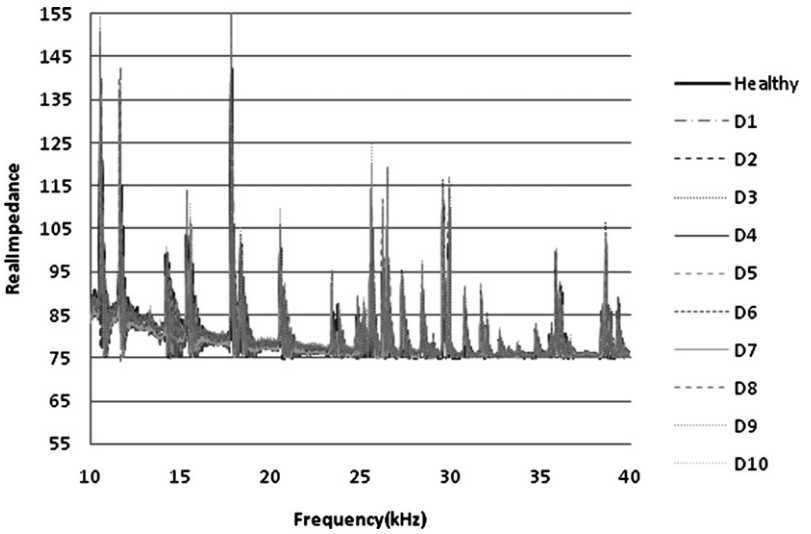

Fig. 8. Comparison of real part of impedance signature resulted from accumulated damages (1 to 10) inserted on Al-thick hollow cylinder.

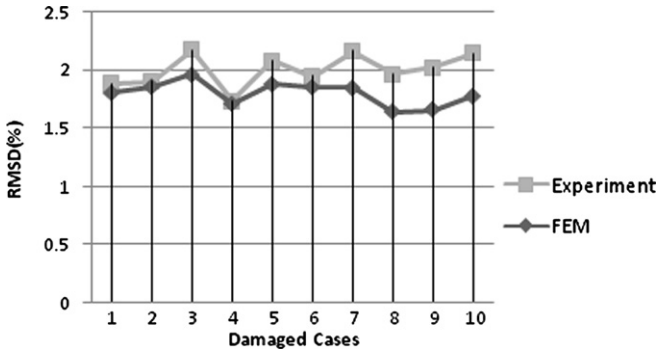

Fig. 9. Comparison of RMSD values obtained by experimental test and by FEM simulation for the thick aluminum specimen.

The resulted RMSD trends presented in Fig. 9 are related to the Al-thick cylinder. To examine if different specimen materials with similar accumulative damages vary RMSD trends, an additional investigation is required. For this purpose, the specimens with different mechanical properties and thicknesses were tested both by experiments and FEM. Mechanical stiffness k can be described by Eqs. (7) and (8):

$$k = \frac{F}{\delta} \tag{7}$$

$$k = \frac{A.E}{L} \tag{8}$$

Here, F is the applied load and δ is the resultant displacement. A is the cross section are, L is the element length and E is the Young modulus.

To explore the influence of thickness and mechanical properties of cylinders on damage metrics by EMI technique and in addition to Al-thick cylinders, similar tests were carried out on Al and steel thin/thick cylinders according to Table 4. Fig. 10 shows damage metrics resulted from accumulated damages inserted on these test specimens.

It can be seen that for thick and stiffer specimens (ex: St-thick), damage metric levels are lower than thin specimens with less stiffness as described in Eq. (8). The results demonstrate that damage metrics by EMI technique are not only affected by damage intensity but also by stiffness of specimen material and the thickness. This was expected from Eq. (1). In fact, the mechanical impedance of both structure and sensor is related to the stiffness of structure and sensor in a 1-dimensional model by Eq. (9):

$$Z(\omega) = \frac{F(\omega)}{v(\omega)} = \frac{k}{j\omega} \tag{9}$$

$F(\omega)$ is the applied load in each frequency and $v(\omega)$ is the resultant velocity of system. k is mechanical stiffness and ω is the angular frequency. Since mechanical impedance $Z_{str}(\omega)$ is the ratio of excitation force to induced velocity, it directly

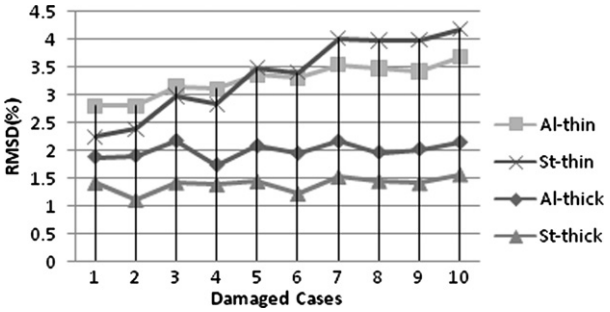

Fig. 10. RMSDs related to accumulated damages (1 to 10) inserted on aluminum and steel specimens (specified in Table 4) obtained by experimental tests.

affects electrical impedance of the PWAS. Therefore, any changes in the stiffness of structure such as damage, specimen thickness and Young modulus of specimen material, influence the monitored impedance spectrum.

In addition, as the inserted damages with similar intensity in thin specimens generate a greater ratio of damage depth to specimen thickness, it can be observed that damage metric levels are higher for thin specimens. However, in the literature, the intensity of damage is referred to the geometrical dimensions of damage itself [2,17], whereas, in fact, the intensity of damage relative to host structure thickness should be considered in damage metrics analysis too.

6. Conclusion

Damage detection of hollow cylinders by the EMI technique was performed on aluminum and steel specimens with different thicknesses. Finite Element Model of the EMI technique on hollow cylinders was developed and validated in order to study the influence of different damage types and damage location on EMI spectrum and resultant damage metrics.

Experimental and simulation results show that both orientation and longitudinal distance from sensor location affect the damage metrics. Circumferential damages located on the opposite side of PWAS position and near sensor location have a higher effect on the damage metrics. This is about 5% for circumferential damages and up to 10% for longitudinal damages.

Accumulating damage on hollow cylinders does not always lead to an increase in damage metrics using the RMSD algorithm. Therefore, to distinguish each of these sequentially accumulated damages will not be an easy task. The results demonstrate that damage metrics by EMI technique are not only affected by damage intensity in each specimen but also by mechanical properties of specimen material and the thickness. Finite Element Model developed in this study can be utilized to predict the EMI spectrum and the resultant damage metrics. It will be particularly useful for complex structures where the integrity of these structures is affected by damages.

References

[1] N. Sepehry, M. Shamshirsaz, A. Bastani, Experimental and theoretical analysis in impedance-based structural health monitoring with varying temperature, Structural Health Monitoring 10 (2011) 573–585.
[2] G. Park, H. Sohn, C.R. Farrar, D.J. Inman, Overview of piezoelectric impedance-based health monitoring and path forward, The Shock and Vibration Digest 35 (2003) 451–463.
[3] Andrew B. Thien, Pipeline structural health monitoring using macro-fiber composite active sensors, Master's thesis, Research and Advanced Studies of the University of Cincinnati, 2006.
[4] C. Liang, F.P. Sun, C.A. Rogers, Coupled electro-mechanical analysis of adaptive material systems – Determination of the actuator power consumption and system energy transfer, J. Intell. Mat. Syst. Struct. 5 (1994) 12–20.
[5] K.H. Tseng, C.K. Soh, A.S.K. Naidu, Non-parametric damage detection and characterization using smart piezoceramic material, Smart Mater. Struct. 11 (2002) 317–329.
[6] V. Giurgiutiu, A. Zagrai, Characterization of piezoelectric wafer active sensors, J. Intell. Mat. Syst. Struct. 11 (2000) 959–976.
[7] A.N. Zagrai, V. Giurgiutiu, Electro-mechanical impedance method for notch detection in thin plates, J. Intell. Mat. Syst. Struct. 12 (2001) 709–718.
[8] V. Giurgiutiu, A. Zagrai, Damage detection in thin plates and aerospace structures with the electro-mechanical impedance method, Structural Health Monitoring 4 (2) (2005) 99–118.
[9] C.K. Soh, K. Tseng, S. Bhalla, A. Gupta, Performance of smart piezoceramic patches in health monitoring of a RC bridge, Smart Mater. Struct. 9 (2000) 533–542.
[10] S. Bhalla, A.S.K. Naidu, C.K. Soh, Influence of structure-actuator interactions and temperature on piezoelectric mechatronic signatures for NDE, LA-UR-03-1467, Proceedings of SPIE – The International Society for Optical Engineering 5062 (1) (2002) 263–269.
[11] S. Zhou, C. Liang, C.A. Rogers, Modeling of distributed piezoelectric actuators integrated with thin cylindrical shells, J. Acoust. Soc. Am. 96 (3) (1994) 1605–1612.
[12] Y.W. Yang, J.F. Xu, C.K. Soh, Generic impedance-based model for structure-piezoceramic interacting system, J. Aerosp. Eng. 18 (2005) 93–101.
[13] Yaowen Yang, A. Yuhang Hu, Electromechanical impedance modeling of PZT transducers for health monitoring of cylindrical shell structures, Smart Mater. Struct. 17 (1) (2008) 015005, 11 pp.
[14] K. Tseng, P.K. Basu, L. Wang, Damage identification of civil infrastructures using smart piezoceramic sensors, in: Proceedings of the First European Workshop on Structural Health Monitoring, 2002, pp. 450–457.
[15] Daniel M. Peairs, Daniel J. Inman, Gyuhae Park, Circuit analysis of impedance-based health monitoring of beams using spectral elements, Structural Health Monitoring 6 (2007) 81–94.
[16] N. Sepehry, M. Shamshirsaz, F. Abdollahi, Temperature variation effect compensation in impedance-based structural health monitoring using neural networks, J. Intell. Mat. Syst. Struct. 22 (2011) 1975–1982.

[17] Victor Giurgiutiu, Structural Health Monitoring with Piezoelectric Wafer Active Sensors, Academic Press, 2005.
[18] G.L. Wojcik, D.K. Vaughan, N.N. Abboud, J. Mould Jr., Electromechanical modeling using explicit time-domain finite element, in: IEEE Ultrasonic Symposium Proc., vol. 2, 1993, pp. 1107–1112.
[19] ABAQUS Inc., Analysis user's manual, Version 6.9, Providence, RI, 2009.
[20] S. Zhou, C. Liang, C.A. Rogers, A dynamic model of piezoelectric actuator-driven thin plates, in: Proc. Smart Structures and Materials Conf. (Orlando), Proc. SPIE 2190 (1994) 550, http://dx.doi.org/10.1117/12.175216.